FOREX Publication
Open Access | Rapid and quality publishing

International Journal of
Electrical and Electronics Research (IJEER)
Research Article | Volume 12, Issue 4 | Pages 1351-1356 | e-ISSN: 2347-470X

Leveraging Hybrid Precoding for Enhanced Terahertz Communication System

T.Srilatha[1], Pinjala N Malleswari[2], Durgachandramouli Y[3], T J V Subrahmanyeswara Rao[4], and M. Ravisankar[5]

[1]*Department of ECE, Vignan's Institute of Engineering for Women,Vishakapatnam, India; srilathamellum@gmail.com*
[2]*Department of ECT, Sasi Institute of Technology & Engineering, Tadepalligudem, India; pinjalamalleswari@gmail.com*
[3]*Department of ECE, Aditya College of Engineering and Technology, Surampalem, India; yd.chandramouli@gmail.com*
[4]*Department of ECE, Sasi Institute of Technology & Engineering, Tadepalligudem, India; tjvsrao@gmail.com*
[5]*Department of ECE, Sasi Institute of Technology & Engineering, Tadepalligudem, India; mravi@sasi.ac.in*

***Correspondence:** *pinjalamalleswari@gmail.com;*

ABSTRACT- Terahertz (THz) transmission is a promising strategy for future 6G networks, offering ultra-wide bandwidth. Effective channel modeling and precoding techniques are essential for achieving required coverage and addressing significant path loss in THz communications. In this paper, we comprehensively examine the major THz precoding algorithms for future 6G networks, focusing on their significant challenges and prospects. We discriminate between millimeter-wave and THz channels and uncover issues with THz precoding, such as distance-dependent direction loss, beam split impact, and excessive power usage. To solve these issues, three distinct THz precoding systems, such as hybrid precoding, analog beamforming, and delay-phase precoding, are introduced and their performance is compared.

Keywords: Terahertz communication, 6G Networks, Millimeter-wave, Precoding System, Beam forming.

ARTICLE INFORMATION

Author(s): T.Srilatha, Pinjala N Malleswari, Durgachandramouli Y, T J V Subrahmanyeswara Rao, and M. Ravisankar;
Received: 10/09/24; **Accepted:** 15/11/24; **Published:** 15/12/24;
E- ISSN: 2347-470X;
Paper Id: IJEER240421;
Citation: 10.37391/ijeer.120428
Webpage-link:
https://ijeer.forexjournal.co.in/archive/volume-12/ijeer-120428.html

Publisher's Note: FOREX Publication stays neutral with regard to jurisdictional claims in Published maps and institutional affiliations.

1. INTRODUCTION

Terahertz (THz) communication Systems operate between 0.1 to 10 THz, providing ultra-wide bandwidth and a high data rate for 6G communication. THz communication's short wavelength allows excellent spatial resolution and fast data transmission for applications including streaming ultra-high-definition video, real-time VR/AR, and wireless backhaul for dense networks. The method is excellent for short-range, line-of-sight communication owing to substantial air absorption and dispersion of THz signals. Efficacy and propagation issues are generally addressed using advanced antenna arrays and beamforming.

Jingbo et al. provided the limitations of the 5G millimeter wave spectrum and the importance of THz precoding. 5G spectrum cannot accommodate a large data rate. Path loss (120 dB/100 m at 0.6 THz) makes terahertz (THz) transmissions difficult. This loss makes coverage difficult. Precoding may minimize this without boosting transmit power. Therefore, THz precoding is essential for future 6G networks [1]. Yan et al. designed the THz hybrid precoding technique, which combines digital and analog precoding, is an economical and adaptable system that trades performance and power usage [2]. Zhang et al. studied an approach mMIMO-ISAC (Integrated sensing and massive multiple-input multiple-output (MIMO) communication) at THz bands. The technique links channel and target parameters across angular, delay, and Doppler domains by using the sparse nature of THz channels. Tensor-based strategies are used to predict these parameters. The findings show that the method considerably lowers training overhead while achieving target estimate accuracy close to ideal [3]. To overcome the difficulties of a fully digital precoding technique, many authors proposed cutting RF chains using analog components, linking many antennas, and guiding beams with phase shift networks. Though analog precoding uses less power, phase shifts are quantized, limiting support to one data stream [4-6].

Emerging beam array gain depends on antenna array size. THz communication requires huge antenna arrays due to its short wavelength.6G networks need THz precoding to improve route loss. The specific properties of 6G precoding provide additional obstacles that must be overcome for a viable 6G system [7-10]. Huq et al. and Busari et al. developed a network communication scheme with cost efficiency, computation complexity, and minimum energy feasting [11-12]. Ayach et al. [13] offered a hybrid precoding, which combines analog beam formers and digital processing with fewer RF chains. It achieves full array gain by steering narrow beams from analog beam formers to target users. Wnag et al. [14] designed a massive MIMO channel model to address

FOREX Publication
Open Access | Rapid and quality publishing
International Journal of Electrical and Electronics Research (IJEER)
Research Article | Volume 12, Issue 4 | Pages 1351-1356 | e-ISSN: 2347-470X

frequency- and spatial-wideband effects, how they affect transceiver design, and how they interact with frequency selectivity in multi-carrier modulations such as OFDM.

Busari et al. [15] proposed a fully-adaptive RA for a dense, C-RAN-enabled mmWave massive MIMO network. Its performance is compared with a non-adaptive and two semi-adaptive RA schemes. The proposed scheme outperforms all the other RA schemes. Park et al. [16] developed a closed-form solution for fully connected OFDM-based hybrid analog/digital precoding for frequency-selective mmWave systems. Cai et al. [17] explored beam squint in uniform linear arrays (ULAs) and its effects on codebook design, focusing on the number of antennas and system bandwidth relative to carrier frequency. Phase shifters in 5G mmWave massive MIMO concentrate beams from various sub-carriers in opposite directions, reducing array gain. Beam squint effects reduce array gain, hence several methods are used by researchers [18-20].

In wireless communications, THz is a potential alternative for Tbps communications given current hardware and signal-processing capabilities. Scarcity of sub-6 GHz spectrum: Advanced transmission systems like MMIMO [21], NOMA [22], and THz propagation channel characteristics are addressed in [23]. For Tbps communications, massive frequencies beyond 100 GHz are required. Challenges in optical bands: Despite the wide range of IR [24], visible light [25], and UV frequencies [26]. Akyildiza et al. [27] analyzed the limitations and potential resolutions for high-speed transceiver structural design. Jiang et al. [28] addressed the difficulties by making 6G and future mobile technology adoption. This review presented an ultrahigh band health risks: By dislodging electrons and creating free radicals, UV, X-rays, and Gamma rays may cause cancer. Ionizing radiation is used in radiotherapy, photography, semiconductor manufacture, and nuclear medicine.

In this investigation, we applied DPP (delay phase precoding) with different transmitting antennas like 256, 512, and 1024 for a fixed number of receiving antennas 4 including various time delay elements 4,8,16, and 32. The experimental results are compared in both THz and mmWave communication.

2. PRECODING TECHNIQUES

In precoding, we analyze the multi-carrier system, where an AP equipped with N_t antennas communicate *via* $'N'$ subcarriers and N_{RF} RF chains. The transmitted signal at each subcarrier is represented by equation (1).

$$x(n) = E_{RF}E_{BB}[n]s[n],\ for\ n = 1,2,3 \ldots\ldots N. \quad (1)$$

Where $s = [s_1, s_2, \ldots s_N]^T$ indicates the data symbols at subcarrier *n*.

2.1 RIS based Precoding

The RIS acts as a reflecting array, introducing analog beamforming to impinge signals. This simplifies architecture, reduces costs, and improves beamforming performance for THz communication systems.

$$y_n = (g_n^T \prod_{n=1,2--N} \emptyset_n H_n + w_n)s_n + m_n \quad (2)$$

Where $g_n \in C^{N_{RF}\times 1}$ & $w_n \in C^{1\times N}$ indicate the channel from the last RIS to the n^{th} user and the direct channel from the BS to user n, $\emptyset_n \triangleq diag[\theta_{n1}, \theta_{n2}, ---\theta_{nN} \in C^{N_i\times N_i}]$ is the phase shift matrix of the n^{th} RIS, $s_n \in C^{N\times 1}$ is the transmit vector from the BS and m_n is noise vector [29].

2.2 NF-based Precoding

The received signal may be represented as

$$y_n = H_n F_A F_D s_n + m_n \quad (3)$$

Where y_n is $the\ N_r \times 1$ vector, H_n is $N_r \times N_t$ channel matrix, and m_n is the noise component [30].

2.3 Delay Phased Precoding

The architecture of the DPP network is presented in Figure 1. For beamforming, the system demonstrates data flow from baseband processing to several RF chains, each bonded to a TD network, so that the system can steer the signal directionality across sub-arrays, like sub-arrays 1 through K. The digital signals are modulated and encoded by the baseband processing block before being sent to the RF chains. RF chains transform baseband signals into RF signals for every data stream. Time delays are used in TD Networks to beam form radio frequency signals to pre-selected sub-arrays according to time and phase. Sub-arrays are transmitting and receiving arrays of antennas. They are used to increase directional performance and spatial signal processing.

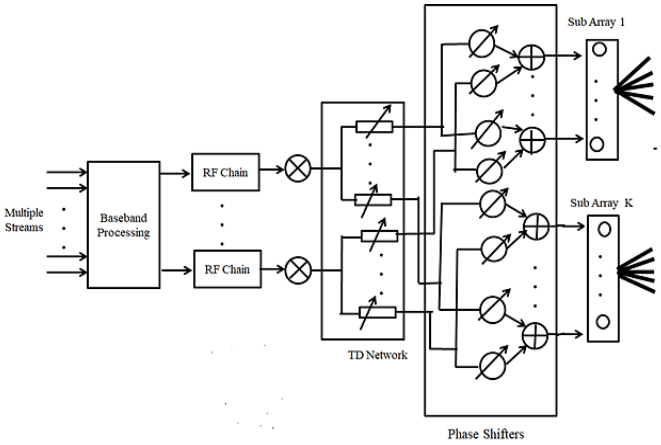

Figure 1. The proposed DPP network [1]

The proposed algorithm steps are outlined as follows:
Step 1: Set input variables and system parameters with their initial values.

Step 2: Represent the channel and its input signal.

Step 3: Obtain the n^{th} subcarrier channel $H_n \epsilon C^{N_t\times N_r}$.

FOREX Publication
Open Access | Rapid and quality publishing
International Journal of Electrical and Electronics Research (IJEER)
Research Article | Volume 12, Issue 4 | Pages 1351-1356 | e-ISSN: 2347-470X

Step 4: Construct the analog beam former $F_{RF_m} \epsilon C^{N_t \times N_{RF}}$ and is given by *equation (4)*.

$$F_{RF_m} = \left[F_{RF_{m,1}}, F_{RF_{m,2}}, \ldots . F_{RF_{m,N_{RF}}}\right] \quad (4)$$

Step 5: Obtain the Block diagonal representation of $F_{RF_{m,p}}$ and is given by *equation (5)*, which is linked with p^{th} RF chain through TDs

$$F_{RF_{m,p}} = blkdig([\overline{a_{p,1}}, \overline{a_{p,2}}, \overline{a_{p,3}} \ldots \overline{a_{p,k}}]) \quad (5)$$

Step 6: Describe the phase shift $A_n^{TD} \epsilon C^{KM_{RF} \times M_{RF}}$, which depends on frequency and is given by *equation (6)*

$$A_n^{TD} = blkdiag([e^{-j2\pi f_n t_1, -j2\pi f_n t_2, \ldots, -j2\pi f_n t_{N_{RF'}}}]) \quad (6)$$

Step 7: Define the baseband precoder $F_{BB_n} \epsilon\, C^{N_{RF} \times N_s}$ at the n^{th} subcarrier.

Step 8: Obtain the received signal y_n , which is the combination of beamforming and precoding effects given by *equation (7)*

$$y_n = H_n^H \sum_{m=1}^{N} F_{RF_m} A_n^{TD} f_n^{BB} s_n + m_n \quad (7)$$

Where m_n an AWGN (additive white gaussian noise) indicates is given by $m_u \epsilon\, N_r \times 1$.

3. IMPLEMENTATION RESULTS

To compare the feasible sum rate of used precoding methods, including the optimal fully-digital precoding simulation data are presented. The used THz system has a bandwidth of 5 GHz and a carrier frequency of 0.14 THz. The AP includes a 256-element ULA to serve several users.

The simulation settings are displayed in *Table 1.*

Table 1. Simulation settings

Parameters	Values
No of transmitting antennas N_t	256,512, and 1024
No of receiving antennas Nr	4
No of channel paths L	1
central frequency fc	0.14 THz, 28GHz
Bandwidth B	5 GHz
No of subcarriers M	128
No of RF chains NRF	4
No of Time Delay elements	K=4,8,16,32
SNR	-20 dB to 20dB
Physical directions of the paths θ_l, φ_l	U[π/2, π/2]

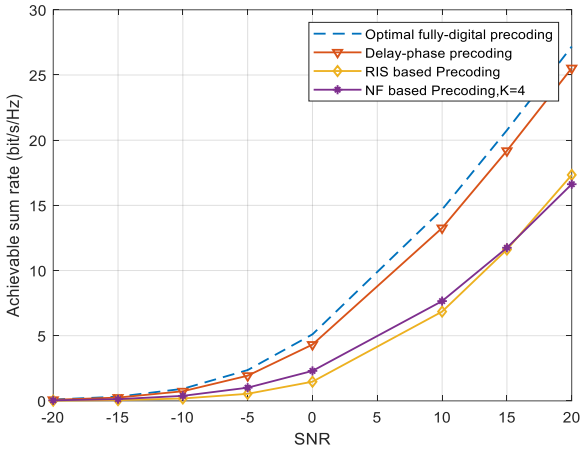

Figure 2. Sum rate vs SNR for K=4

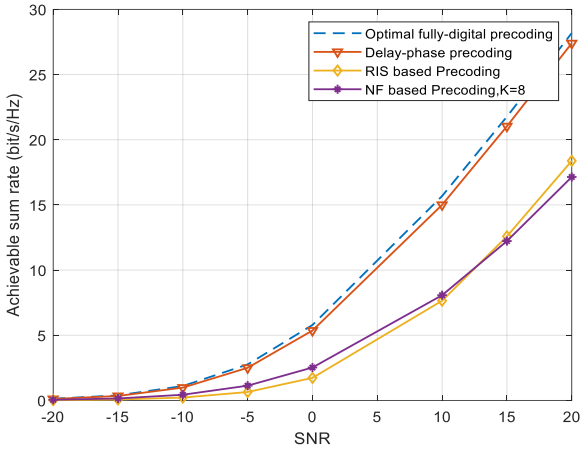

Figure 3. Sum rate vs SNR for K=8

From *figure 2* to *figure 5*, the proposed DPP's attainable sum rate, RIS, and NF-based precoding have been compared with different time delayers, K=4,8,16, and K=32. We conclude that this DPP approach far exceeds earlier techniques, achieving 94% of the optimal precoding due to combined delay-phase control.

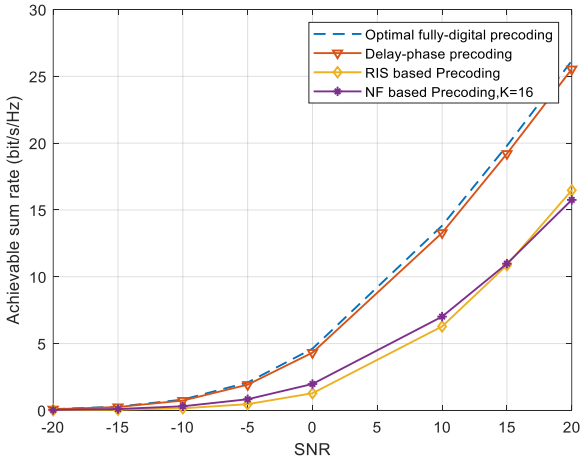

Figure 4. Sum rate vs SNR for K=16

FOREX Publication
Open Access | Rapid and quality publishing
International Journal of Electrical and Electronics Research (IJEER)
Research Article | Volume 12, Issue 4 | Pages 1351-1356 | e-ISSN: 2347-470X

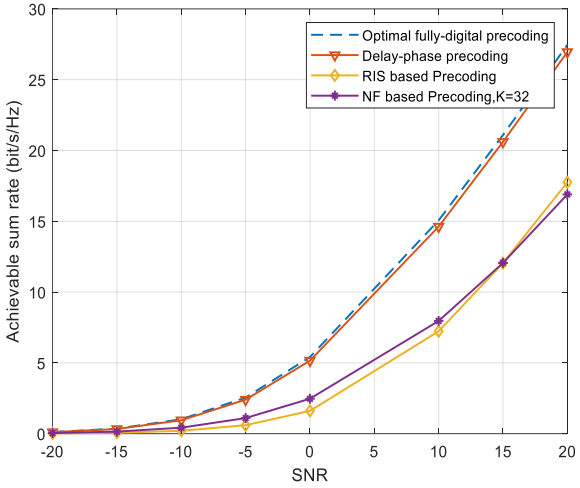

Figure 5. Sum rate vs SNR for K=32

For K= 4, the recommended DPP achieves a sum rate of 25.9 bits/s/Hz, which is close to optimum precoding (94%) at 27.37 bits/s/Hz.For K= 8, the sumrate is 25.1bits/s/Hz for DPP, which is near optimum precoding (91.2%) at 27.3bits/s/Hz. For K=16, the DPP sum rate value is 21.01bits/s/Hz, nearby optimum precoding (71%) at 27.01bits/s/Hz. For K=32, the DPP accomplishes a sum rate of 16.08 bits/s/Hz, which is close to optimum precoding(43%) at 25.61 bits/s/Hz. The comparative analysis of various precoding techniques for 20dB SNR is presented in *table 2*.

Table 2. Comparison of several precoding techniques achievable sum rate at SNR= 20dB

Precoding method	No of Delays	Number of Antennas		
		256	512	1024
Optimal	K=4	27.37	27.98	28.0
	K=8	27.3	27.57	27.9
	K=16	27.01	26.9	27.6
	K=32	25.61	26.5	27.2
RIS Based	K=4	10.46	14.9	18.1
	K=8	10.17	14.7	17.9
	K=16	10.17	14.46	17.8
	K=32	10.06	13.9	17.7
NF based	K=4	8.33	12.39	17.6
	K=8	8.19	12.31	17.2
	K=16	7.65	11.8	17.0
	K=32	7.62	11.8	16.8
Proposed Delay Phase	K=4	25.9	27.2	27.3
	K=8	25.1	26.7	27.1
	K=16	21.01	25.9	26.9
	K=32	16.08	22.26	26

Similarly, the proposed DPP with N=1024 outperforms existing approaches, such as RIS and NF-based precoding, as illustrated in *figures 3 to 5*. In all precoding techniques, increasing the number of transmitting antennas from N=256 to 1024 boosts the achievable sum rate.

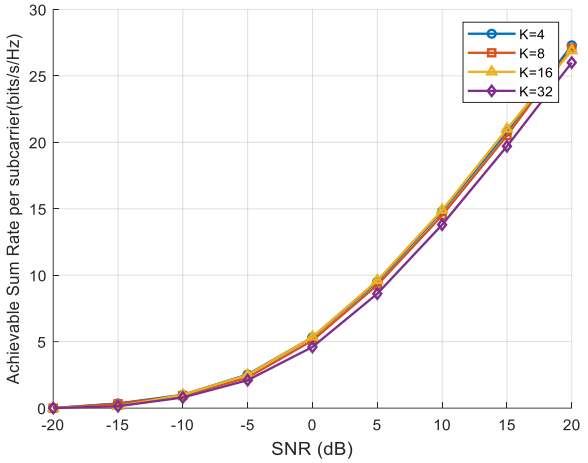

Figure 6. Various time delayers comparison

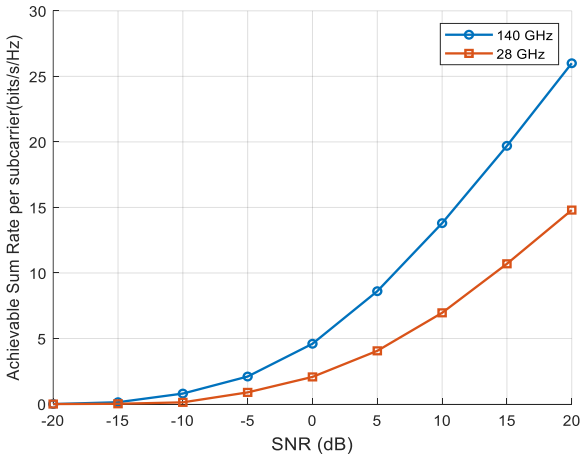

Figure 7. THz vs mmWave channel achievable sum rates

Figure 6 compares the effectiveness of the proposed DPP network by several time delayers. The comparison displays that K=4 and K=8 have larger values than K=16 and K=32. To construct the recommended network, the optimal number of time delayers in the design must be smaller, such as K=16 or K=32, rather than K=4 or K=8. *Figure 7* compares the proposed DPP network's performance in the THz and mmWave channels. It has been shown that its efficiency is far superior at *f=0.14* THz (sub-THz channel) than at *f=28* GHz (mmWave channel). For THz channels, the recommended network effectively eliminates the beam split impact caused by ordinary phase shifters, significantly improving the performance rate; however, in mmWave channels, the projected network is unable to completely eradicate the beam squint effects.

FOREX Publication
Open Access | Rapid and quality publishing
International Journal of Electrical and Electronics Research (IJEER)
Research Article | Volume 12, Issue 4 | Pages 1351-1356 | e-ISSN: 2347-470X

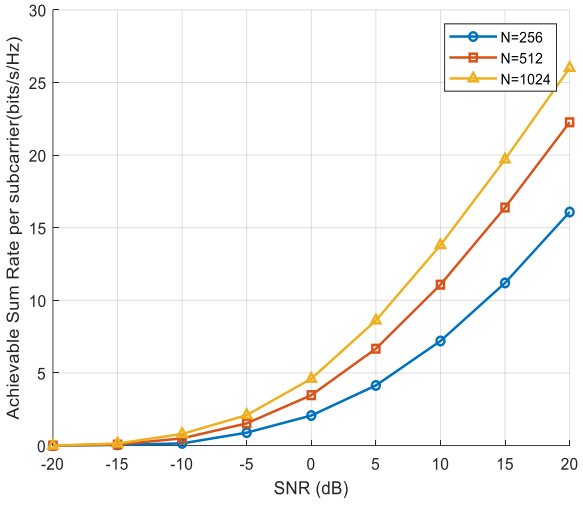

(a)

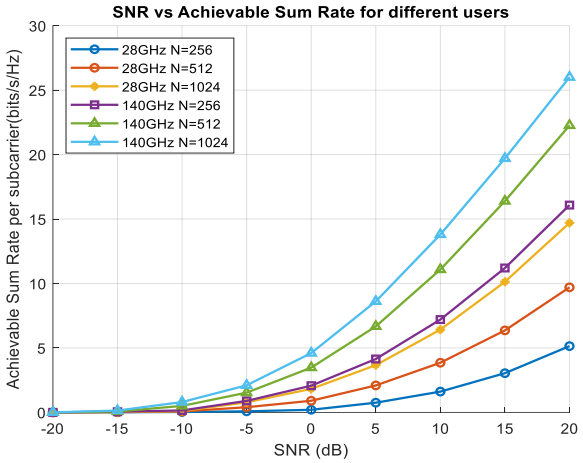

(b)

Figure 8. Comparative analysis of rate efficiency for various antenna counts in (a) mm-wave (b)THz channel

Figure 8(a) associates the results of the intended DPP with varying numbers of AP antennas. There is little variation detected when the value of N is changed. The best performance is seen when N = 1024. As a result, the DPP is capable of addressing the attainable rate deterioration caused by the beam split effect, as well as achieving more optimum achievable rate efficiency. *Figure 8(b)* demonstrates that the THz frequencies and a larger number of subcarriers afford superior performance in terms of achievable sum rate per subcarrier. For example, the sum rate of mmWave is 14.7bits/s/Hz, but for the THz channel is 26bits/s/Hz, which is increased by 76.87% with K=4.

3.1 Performance Evaluation

The efficiency of the system is measured with SE [bits/s)/Hz] per user, which is calculated by *equation (7).*

$$SE_n = log_2(1 + SNR_n) \quad (7)$$

Where SNR_n is signal to noise ratio for each user. The achievable sum rate of the system is given by *equation (8).*

$$R = \sum_{n=1}^{N}(BW_n \; X \; SE_n) \quad (8)$$

Where BW_n is the allocated bandwidth per user.

4. CONCLUSIONS

The present research evaluated the downlink single cell AP linked to many users for the 6G indoor office network implementation scenario, and it defines the channel model and antenna parameters. The suggested DPP methodology is employed to adjust for the beam split effect, and its effectiveness is assessed with RIS and NF-based precoding applying typical frequency-independent phase shifters. According to simulated results and theoretical research, this DPP technique is capable of eliminating the beam split phenomenon while achieving a higher rate performance (94%) for K=4 with N=256 antennas. The effects of carrier frequencies of 28 GHz mmWave and 140 GHz, the quantity of transmitting antennas, and time delayers on achievable total rate performance for a single cell multi-user setup were investigated using the DPP Technique. This investigation is going to be expanded for multi-cell circumstances in the future.

5. ACKNOWLEDGMENTS

Our thanks to the management of Sasi Institute of Technology and Engineering, Tadepalligudem, Andhra Pradesh, who have contributed towards development of the work.

REFERENCES

[1] Jingbo, T.; Linglong, D. THz Precoding for 6G: Challenges, Solutions, and Opportunities. IEEE Wire.Comm., August 2023; pp.132-138.

[2] Yan, L.; Han, C.; Yuan, J. A dynamic array-of-subarrays architecture and hybrid precoding algorithms for terahertz wireless communications. IEEE Jour. On Sele.Areas in Comm., 2020; vol.38, no.9, pp.2041–2056.

[3] Zhang, R.; Wu, X.; Lou, Y.; Yan, F. G.; Zhou, Z.; Wu, W.; Yuen, C. Channel training-aided target sensing for terahertz integrated sensing and massive MIMO communications. IEEE Internet of Things Journal, 2024.

[4] Dai, M.; Clerckx, B. Hybrid precoding for physical layer multicasting. IEEE Comm. Lett., 2016; vol.20, no.2, pp.228–231.

[5] Lin, C.; Li, G. Terahertz communications: An array-of subarrays solution. IEEE Comm. Mag., 2016; vol.54, no.12, pp.124–131.

[6] Venkateswaran, V.; Van der Veen, A.J. Analog beamforming in MIMO communications with phase shift networks and online channel estimation. IEEE Trans. on Sig. Proce., 2010; vol.58, no.8, pp.4131–4143.

[7] Jeyakumar, P.; Ramesh, A.; Srinitha, S.; Vishnu, V.; Muthuchidambaranathan, P. Wideband hybrid precoding techniques for THz massive MIMO in 6G indoor network deployment. Telecommunication Systems, 2022; vol.79, no.1, pp.71-82.

[8] Busari, S.; Huq, Kazi, M. S.; Mumtaz, S.; Dai, L.; Rodriguez, J. Millimeter-wave massive MIMO communication for future wireless systems: A survey. IEEE Comm.Surv.Tuto., 2017; vol. 20, no.2, pp.836-869.

[9] Alkhateeb, A.; Leus, G.; Heath, R. W. Limited feedback hybrid precoding for multi-user millimeter wave systems. IEEE Trans.Wire.Comm. 2015; vol.14 no.11, pp.6481-6494.

[10] Chih-Lin, I. Seven fundamental rethinking for next-generation wireless communications. APSIPA Trans. on Sig. and Infor.Proce., 2017; 6, e10.

[11] Huq, K. M. S.; Mumtaz, S.; Bachmatiuk, J.; Rodriguez, J.; Wang, X.; Aguiar, R. L. Green HetNetCoMP: Energy efficiency analysis and optimization. IEEE Trans. on Veh. Tech., 2014; vol. 64, no.10, pp.4670-4683.

[12] Busari, S. A.; Huq, K. M. S.; Felfel, G.; Rodriguez, J. Adaptive resource allocation for energy-efficient millimeter-wave massive MIMO networks. IEEE Glob. Comm. Conf., 2018; pp. 1-6.

[13] Ayach, O. E.; Rajagopal,S.; Abu-Surra,S.; Pi,z.; Heath, R.W. Spatially sparse precoding in millimeter wave MIMO systems. IEEE Trans. on Wire. Comm.., 2014; vol. 13, no. 3, pp. 1499–1513.

[14] Wang, B.; Gao, F.; Jin, S.; Lin, H.; Li, G. Y.; Sun, S.; Rappaport, T. S. Spatial-wideband effect in massive MIMO with application in mm Wave systems. IEEE Comm. Mag.., 2018; vol. 56, no. 12, pp. 134–14.

[15] Park, S.; Alkhateeb, A.; Heath, R. W. Dynamic subarrays for hybrid precoding in wideband mmWave MIMO systems. IEEE Trans. on Wire. Comm., 2017; vol. 16, no. 5, pp. 2907–2920.

[16] Kong, L.; Han, S.; Yang, C. Hybrid precoding with rate and coverage constraints for wideband massive MIMO systems. IEEE Trans. on Wire. Comm., 2018; vol. 17, no. 7, pp. 4634– 4647.

[17] Cai, M.; Gao, K.; Nie, D.; Hochwald, B.; Laneman, J. N.; Huang, H.; Liu, K. Effect of wideband beam squint on codebook design in phased-array wireless systems. IEEE Glob. Comm. Conf., 2016; pp. 1–6.

[18] Liu, X.; Qiao, D. Space-time block coding-based beamforming for beam squint compensation. IEEE Wire. Comm. Lett., 2019; vol. 8, no. 1, pp. 241–244.

[19] Demirhan, U.; Alkhateeb, A. Radar aided proactive blockage prediction in real-world millimeter wave systems. IEEE Int. Conf. on Commun. (ICC), 2022, pp. 4547–4552.

[20] Nagatsuma, T.; Ducournau, G.; Renaud, C. Advances in terahertz communications accelerated by photonics. Nature Photon, 2016; vol. 10, no. 6, pp. 371–379.

[21] Jiang, W.; Schotten, H. D. Cell-free massive MIMO-OFDM transmission over frequency-selective fading channels. IEEE Comm. Lett., 2021, vol. 25, no. 8, pp. 2718 – 2722.

[22] Liu, Y.; Yi, W.; Ding, Z.; Liu, X.; Dobre, O. A.; Al-Dhahir, N. Developing NOMA to next generation multiple access: Future vision and research opportunities. IEEE Wire.Comm. Mag., 2022; vol. 29, no. 6, pp. 120–127.

[23] Cai, X.; Cheng, X.; Tufvesson, F. Toward 6G with terahertz communications: Understanding the propagation channels. IEEE Communications Magazine, 2024; vol. 62, no. 2, pp.32-38.

[24] Kahn, J.; Barry, J. Wireless infrared communications. Proc. IEEE, 1997; vol. 85, no. 12, pp. 265 – 298.

[25] Xu, Z.; Sadler, B. M. Ultraviolet communications: Potential and state-of-the-art. IEEE Commun. Mag., 2008; vol. 46, no. 5, pp. 67–73.

[26] Akyildiza, I. F.; Jornet, J. M.; Han, C. Terahertz band: Next frontier for wireless communications. Phy. Comm., 2014; vol. 12, pp. 16 – 32.

[27] Jiang, W.; Zhou, Q.; He, J.; Habibi, M.A.; Melnyk, S.; Absi, M.E.; Leung, V. Terahertz communications and sensing for 6G and beyond: A comprehensive view. IEEE Communications Surveys & Tutorials. 2024.

[28] Huang, C.; Yang, Z.; Alexandropoulos, G. C.; Xiong, K.; Wei, L.; Yuen, C.; Debbah. M. Multi-hop RIS-empowered terahertz communications: A DRL-based hybrid beamforming design. IEEE Jou. on Select.Areas in Comm., 2021; vol. 39, no.6, pp.1663-1677.

[29] Wu, Z.; Cui, M.; Zhang, Z.; Dai. L. Distance-aware precoding for near-field capacity improvement in XL-MIMO. IEEE 95th Vehi.Tech. Conf., 2022; pp.1-5, IEEE.